

A NUMERICAL MODEL FOR TWO-DIMENSIONAL BEACH TRANSFORMATION

By *Tomoya SHIBAYAMA** and *Kiyoshi HORIKAWA***

A simplified simulation model for predicting two-dimensional beach transformation was developed based on the recent results of research works on wave transformation, near bottom velocity and sediment transport. The wave field was calculated by the energy flux method based on either cnoidal or linear wave theory in the offshore zone, and by Mizuguchi's¹⁾ energy dissipation model in the surf zone. The velocity field was calculated by the approximate method of Koyama and Iwata²⁾ using the cnoidal wave profile or by linear wave theory. The sediment transport formula of Shibayama and Horikawa³⁾, which includes the effect of suspended sediment caused by vortices created in the vicinity of ripples, was used to calculate transport rates. The model was found to give reasonable results. The results were compared with various laboratory data and the feasibility of the model was discussed.

1. INTRODUCTION

Surface waves travelling onto a beach cause sediment to be transported parallel to (longshore) and perpendicular to (cross-shore) a shoreline. For longshore sediment transport, the transport rate was usually modeled as the product of sediment volume in motion induced by wave action and transport velocity frequently assumed proportional to the longshore current velocity. The model results for longshore transport has been reasonably good. For cross-shore transport, the estimate of net transport rate is more difficult because net transport rate is the total of onshore-directed transport and offshore-directed transport. In order to estimate these two quantities separately, we have to consider wave asymmetry due to shoaling.

The purpose of the present paper is to propose a predictive numerical model to simulate two-dimensional beach transformation caused by cross-shore sediment transport. In these days many research results has been presented on wave shoaling, wave set-up or set-down, near bottom velocity, wave decay in the surf zone and sediment transport. These results will be tried to be summarized to formulate the numerical model in the following.

Shibayama and Horikawa⁴⁾ and Sunamura⁵⁾ have proposed numerical models on two-dimensional beach transformation, but their formulations were too simplified and could not explain the detailed feature of bottom topography. Mizuguchi and Mori⁶⁾ have proposed a precise numerical model but the calculation procedure could not be continued because of numerical instability. The reason for these results are the following two. The wave field and velocity field in the surf zone has not been modeled satisfactory and the on-offshore sediment transport formula has not yet been established.

* Member of JSCE. Dr. Eng., Lecturer, Dept. of Civil Eng., University of Tokyo (Bunkyo-ku, Tokyo 113)

** Member of JSCE Dr. Eng., Professor and Dean, Faculty of Engineering, University of Tokyo (Bunkyo-ku, Tokyo 113)

2. NUMERICAL MODEL

Figure 1 shows the flow of the computer simulation model for beach transformation. The calculation can be started from an arbitrary initial beach profile. Wave transformation and velocity field are calculated from the incident wave conditions and bottom profile. Mean water level change due to radiation stress distribution is also considered. With these quantities, the sediment transport rate is calculated. Then the beach profile change is calculated using the continuity equation for bed materials.

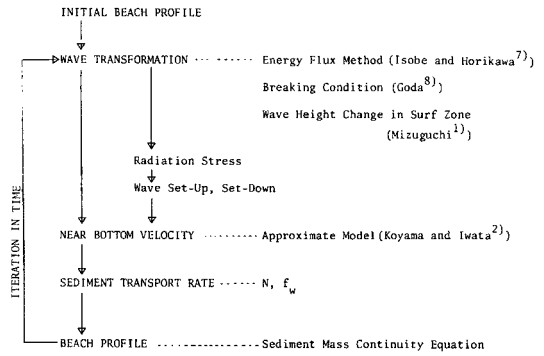


Fig. 1 Procedure of computer simulation.

In order to calculate the sediment transport rate, the time history of the near bottom velocity is required. Therefore, a method to calculate the wave height and near bottom velocity from deep to shallow water should be developed. The wave model, encompassing wave height deformation and the near bottom velocity will be described below. The wave model is only an expedient developed in order to calculate the sediment transport rate. It became apparent that more work needs to be done on wave modeling in the surf zone; however, this was beyond the scope of the present study.

(1) Wave Deformation

The shallow water deformation was divided into three categories; pre-breaking in the offshore region, breaking and post-breaking in the surf zone. The wave transformation in the offshore region was assumed to be given by the energy flux conservation method based on the 1st-order cnoidal wave theory for the region where the Ursell number ($U_r = HL^2/h^3$, H : wave height, L : wave length, h : water depth) was greater than 25 and the 1st-order Stokes wave theory (which is equivalent to linear wave theory) for the region where the Ursell number was equal to or less than 25. The calculation was started by giving the incident wave conditions and local water depth.

In principle, higher-order wave theories should be used. However, it is known that even for higher-order finite amplitude wave theories, for example, the 3rd-order cnoidal wave theory for high Ursell number and the 5th-order Stokes wave theory for low Ursell number, the wave height just before the wave breaking is not well described because the relative wave height H/D (H : wave height, D : average water depth) is too large (Isobe and Horikawa⁷). Therefore, the 1st-order wave theories were considered sufficient for the present purpose.

The wave breaking condition employed is that of Goda⁸

$$H_b/L_0 = 0.17 \{1 - \exp[-1.5 \pi h_b/L_0(1 + 15 i^{4/3})]\} \dots \dots \dots (1)$$

where H_b : the breaking wave height, L_0 : the wave length in deep water, h_b : the water depth at the breaking point and i : the local beach slope. The breaking criteria expressed by Eq. (1) is based on various data as summarized by Goda⁸. Using this criterion, the breaking condition can be determined using the local wave conditions and local bottom profile.

For the wave height decay in the surf zone, the assumption of a constant ratio of wave height to water depth has been used in many applications. This assumption was originally based on observations of wave deformation over a uniformly sloping bottom. For a bar-type beach, this assumption gives an unreasonable wave height distribution.

A more general approach to wave deformation was proposed by Mizuguchi¹¹. In his procedure, the wave height change is given by

$$\frac{d}{dx} (a_i^2 \cdot h^{1/2}) = -\nu_e (4 g^{-3/2} \sigma^2) h^{-1} \dots \dots \dots (2)$$

where a_1 : the wave amplitude, $h' = h + \bar{\eta}$, $\bar{\eta}$: the mean water surface elevation, σ : the angular wave frequency and ν_e : the eddy viscosity which is given by

$$\nu_e = \nu_{eB} (a_1 - c'h') / \gamma'h'^m \dots \dots \dots (3)$$

where $c' = 0.25$, $\gamma' = a_B/h'_B$ and $m = 0.5$. The quantity ν_{eB} is the eddy viscosity at the wave breaking point, which is

$$\nu_{eB} = \frac{5}{2} i \times \frac{gh'_0}{4\sigma} \left\{ 2\pi \left(1 - \frac{c'}{\gamma'} \right) \right\}^{-1/2} \sqrt{L_0/h'_0} \dots \dots \dots (4)$$

(2) Mean Water Level Change

The wave set-up or set-down $\bar{\eta}$ was calculated by the following formula, where S_{xx} is the main component, i. e., the x -direction flux of x -direction-momentum, of the radiation stress :

$$\frac{d\bar{\eta}}{dx} = -\frac{1}{\rho gh'} \frac{dS_{xx}}{dx} \dots \dots \dots (5)$$

The quantity S_{xx} was calculated by the 1st-order cnoidal wave theory or the linear wave theory defined by the local wave height and local water depth.

(3) Near-Bottom Velocity

The maximum values of the onshore-directed and offshore-directed near-bottom velocity, u_{on} and u_{off} , were calculated by using the local wave height and water depth. For the region where the Ursell number was less than 25, the linear wave theory was applied to calculate the water velocity. For the region where the Ursell number was greater than 25, it was found that the velocity obtained with the 1st-order cnoidal wave theory were unrealistically large for the onshore-directed flow. Therefore, an approximate method proposed by Koyama and Iwata²⁾ was applied. According to Koyama and Iwata²⁾, the maximum velocity of the onshore-directed flow, u_{on} , and the offshore-directed flow, u_{off} are given by

$$u_{on} = \frac{2\pi}{T} \frac{\eta_c}{\sinh k(h' + \eta_c)} \dots \dots \dots (6)$$

$$u_{off} = \frac{2\pi}{T} \frac{\eta_t}{\sinh kh'} \dots \dots \dots (7)$$

where η_c : the water elevation at wave crest, k : the wave number and η_t : the water elevation at wave trough. By using the local wave height and water depth, the crest and trough elevation of water surface was calculated by using the 1st-order cnoidal wave theory.

Figure 2 gives a comparison between the 1st-order cnoidal result and the approximate method for a fixed water depth of 20 cm. The approximate method gives lower values than the cnoidal wave for the onshore-directed flow and the value appears to be reasonable. Figure 3 gives comparisons of the present approximate method and the laboratory data. The data were measured by Watanabe et al.⁹⁾ by using hot film anemometer for a fixed bed condition. The experimental condition is shown in Table 1. The horizontal

Table 1 Experimental conditions of Watanabe et al.⁹⁾

Case	h_0 (cm)	T (s)	H_0 (cm)	X_B (cm)	Case	h_0 (cm)	T (s)	H_0 (cm)	X_B (cm)
A-1	24.8	0.80	2.0	47	B-1	44.9	0.80	2.2	23
A-2	24.8	0.80	3.2	82	B-2	44.9	0.80	3.6	38
A-3	24.8	0.80	4.9	112	B-3	45.0	0.80	4.7	48
A-4	24.8	1.00	2.0	57	B-4	44.9	1.00	2.6	33
A-5	24.8	1.00	4.0	102	B-5	44.9	1.00	4.6	53
A-6	24.8	1.00	7.5	172	B-6	44.9	1.00	7.5	84
A-7	24.8	1.24	1.8	62	B-7	44.8	1.24	2.6	35
A-8	24.8	1.24	3.9	102	B-8	44.8	1.24	4.9	63
A-9	24.8	1.24	7.0	162	B-9	44.9	1.24	8.6	88

h_0 : the constant depth in offshore
 T : the wave period H_0 : the deep water wave height
 X_B : the surf zone width

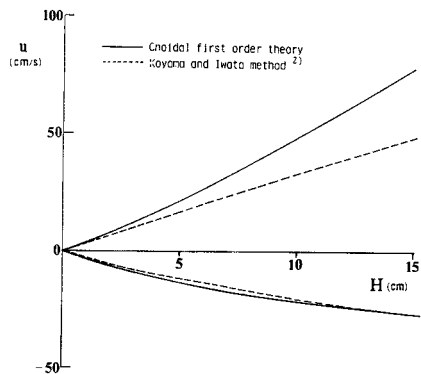


Fig. 2 Near bottom velocity for a given wave height and the water depth of 20 cm.

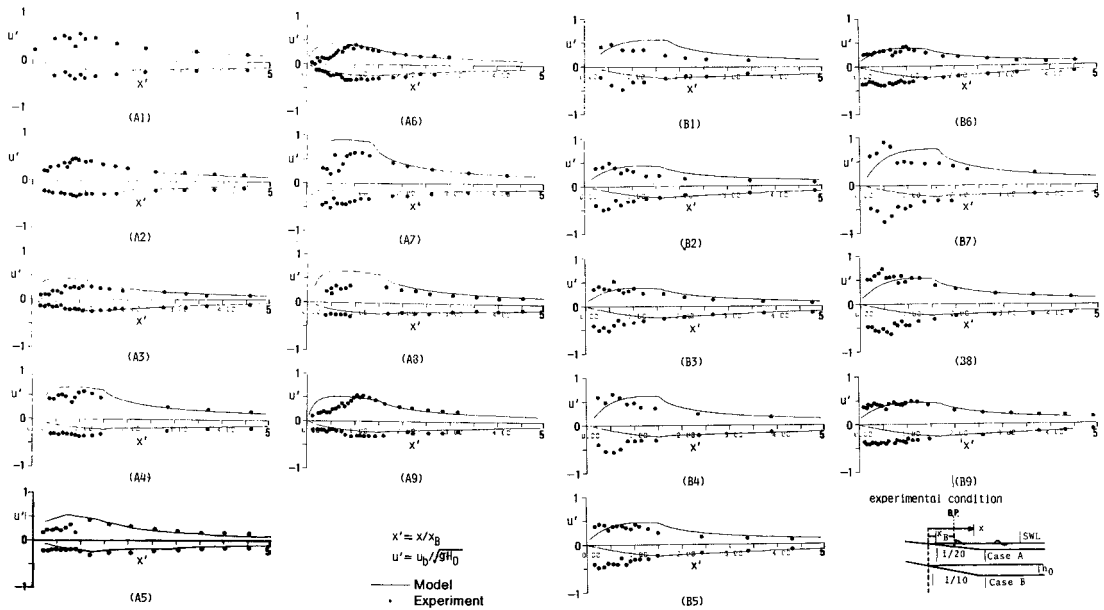


Fig. 3 Model results and measured near bottom velocity (data from Watanabe et al.⁹⁾).

axis is the on-offshore distance x divided by the surf zone width X_B . The vertical axis plots the on-offshore velocity amplitude u_{on} or u_{off} divided by $\sqrt{gH_0}$, where H_0 is the deep water wave height. The calculated velocity in the surf zone somewhat overestimates the value of the onshore-directed flow; however, the difference is not unreasonable due to the following reasons.

In the surf zone, measurements of the velocity field show large fluctuations due to agitation from the breaking waves and resultant turbulent flow, and also due to the effect of the return flow. Moreover, many of the measured values in the former studies were made for a fixed rigid bed, not over a movable sandy bed. Even for a fixed bed, the measured values are not reliable due to the presence of air bubbles created by breaking waves. At present, no wave theory can correctly describe the wave motion and velocity field in the surf zone. Return flow and wave reflection may also be important but are not included in this model. From Fig. 3, we can conclude that the model which is based on the above procedures gives reasonable results for the estimation of the wave motion and velocity field.

(4) Sediment Transport Rate

The sediment transport rate was calculated by using the formulas developed by Shibayama and Horikawa⁹⁾. They classified the sediment transport into three major types and their transient through consideration of dominance of either bed load or suspended load, and of the sediment transport direction. Figure 4 shows their result. The types could be well classified by two parameters, namely, the Shields parameter Ψ_m , which is the nondimensional bed shear stress, the ratio of maximum fluid velocity, u_b , to sediment particle fall

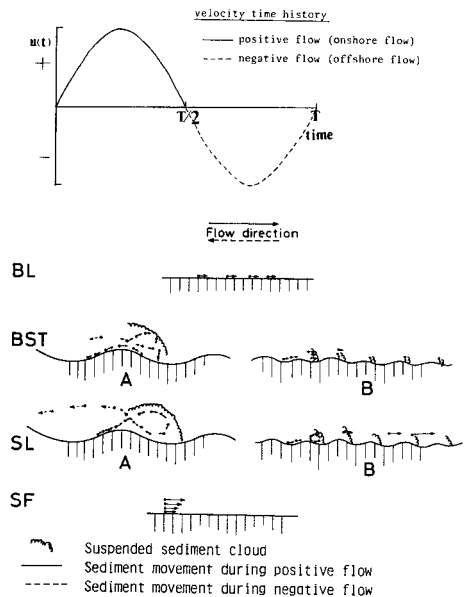


Fig. 4 Sediment transport types.

velocity w . The results are shown in Fig. 5. The definition for Shields parameter is

$$\psi_m = \frac{f_w u_b^2}{2(s-1)gd} \dots \dots \dots (8)$$

where f_w : the Jonsson's wave friction factor, s : the sediment specific gravity and d : the sediment diameter.

In order to divide subtypes A and B, the ratio of water particle orbital diameter to ripple wave length was used. If the ratio is greater than the value three to five, the subtype B appears. Figure 6 shows the relation between the ratio of the ripple wave length, λ , to the water particle orbital diameter, D , and the Shields parameter. Using regression analysis, we get

$$\lambda/D = 1.0 - 0.99 \psi_m^{0.40} \dots \dots \dots (9)$$

Shibayama and Horikawa³⁾ presented simple engineering-oriented formulas for each type of sediment transport. Their results are as follows.

$$\bar{\phi} = 19 \psi_m^3 \text{ for BL, SF, BST-B, SL-B} \dots \dots \dots (10)$$

where $\bar{\phi} = \bar{q}/wd$ and \bar{q} : volumetric rate of sediment transport for a half wave period.

$$\bar{\phi} = -19 N \psi_m^3 \text{ for SL} \dots \dots \dots (11)$$

where $N = D/\lambda$

and

$$\bar{\phi} = (1 - \alpha - N\alpha) 19 \psi_m^3 \text{ for BST-A} \dots \dots \dots (12)$$

where α : the ratio of suspended load originating from the bed load to the total bed load.

Because of wave asymmetry due to shoaling over a sloping beach, the maximum water particle velocity in the onshore-direction is greater than that in the offshore-direction. Since the maximum water particle velocities in the onshore and offshore directions can be calculated individually (Eqs. (6) and (7)), the onshore-directed sediment transport and the offshore-directed sediment transport can be calculated separately. The net sediment transport rate is obtained as the sum of the onshore-directed sediment transport rate and the offshore-directed sediment transport rate.

The transport type was determined by using Fig. 5. Values of α (the ratio of the suspended load which is originated from the bed load to the total bed load) for BST type transport were calculated assuming a linear relationship with the effective Shields parameter. This means that the value of α changes from 0 to 1 in proportion to the Shields parameter in the area of BST transport type, i. e., $\alpha = (\psi_m - \psi_1)/(\psi_2 - \psi_1)$, where ψ_2 is the maximum Shields

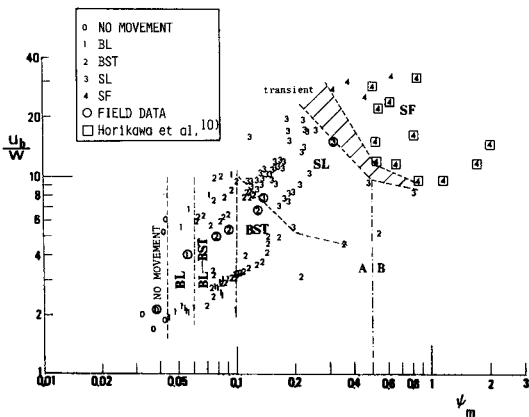


Fig. 5 Transport type classification.

	Sand	Other than Sand
Shibayama and Horikawa ³⁾	b	
Horikawa et al. ¹⁰⁾	c	
Carstens et al. ¹¹⁾	r	1
Shibayama and Horikawa ¹²⁾	s	
Sawamoto et al. ¹³⁾	w	
Kennedy and Falcon ¹⁴⁾	k	2

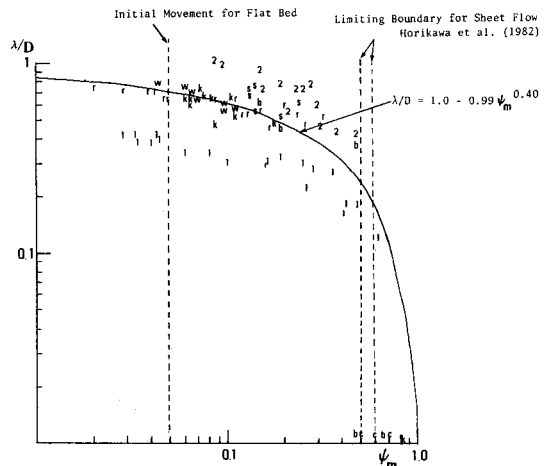


Fig. 6 The correlation between the ratio λ/D , and the Shields parameter.

parameter which corresponds to BST type transport for a specific value of u_b/w , and ϕ_1 is taken as the minimum value for BST transport from Fig. 5. The parameter N denotes the number of ripple lengths over which the cloud travels during a half wave period. The parameter N , the ratio between the water excursion diameter and ripple wave length, was obtained from Eq. (9).

(5) Beach Transformation

The repose angle of a sand bed underwater, β , was given by Gibson (as referred to by Allen⁽⁵⁾), as (d : mm)

$$\tan \beta = 0.47 d^{0.125} (s-1)^{0.19} \dots\dots\dots (13)$$

If during the calculation the local bottom slope became greater than $\tan \beta$, the bottom surface was assumed to become unstable and the average value at two grid points was used. For a dry bed, the pore pressure is not saturated, and therefore we have to consider "cohesive force" between sand particles. According to Terzaghi and Peck⁽⁶⁾, the maximum height of a vertical sand wall under such a condition is given by

$$H_c = N_s c' / \gamma \dots\dots\dots (14)$$

where H_c : the maximum height of a vertical sand wall, $N_s=3.85$, c' : cohesive force, γ : unit weight of sand. The value of c' varies according to the sand diameter and pore pressure. It is impossible to estimate the pore pressure at this time. Therefore the value of H_c was determined as 4 cm for the present case based on the experiments of which condition is listed in Table 2. When the height of vertical sand wall exceeded the value of H_c at the shoreline, the sand wall was assumed to become unstable and the sand level was taken as the average between the two grid points. As a result, the shoreline moved in the onshore direction for an erosional type beach.

(6) Numerical Calculation

In order to employ a finite difference scheme, the study area from the maximum run-up point to the depth of initial movement was divided into 200 intervals of length Δx in the x direction. At each grid point, the wave height, near bottom velocity and sediment transport rate were computed starting from the offshore input (see Fig. 7). The mean surface elevation was calculated by the iteration with the initial value given by the backward Euler method, namely

$$\bar{\eta}(j+1) - \bar{\eta}(j) = \frac{1}{\rho g h'(j)} \{S_{xx}(j) - S_{xx}(j-1)\} \dots\dots\dots (15)$$

where j is the grid number. The bottom elevation was computed by solving the continuity equation for bed materials, in finite difference form, by using the forward Euler method :

$$h(j, k+1) = h(j, k) - \frac{1}{(1-\Lambda)} q_{net}(j, k) \frac{\Delta t}{\Delta x} \dots\dots\dots (16)$$

where q_{net} : the net volumetric sediment transport rate, Λ : the porosity and k : the time step number. The boundaries of sections to apply Eq. (16) were set to be in the middle of grid points. The onshore-directed sediment flux at the grid j affects only to the onshore-directed neighboring section, the center of which is in the grid $j+1$, and the offshore flux to the offshore section of grid $j-1$. This technique makes the calculation to be stable. The detail of the method was described by Shibayama⁽⁷⁾. The time step Δt was selected to be the wave period because the transport formula is based on the time duration of a wave period. The grid interval Δx was selected to be on the order of the ripple wave length because the transport formula describes sediment movement over one ripple.

When the wave height was calculated, the water depth was taken to be the average value of five grid points, i. e., for the grid point j , the water depth was taken as $(h'_{j-2} + h'_{j-1} + h'_j + h'_{j+1} + h'_{j+2})/5.0$.

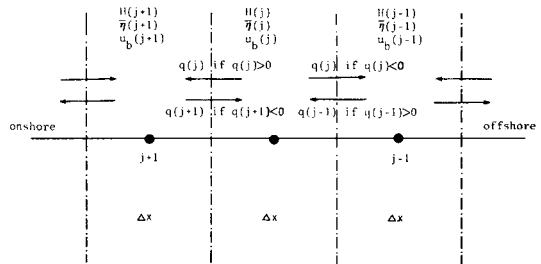


Fig. 7 Computation grid scheme.

where j is the number of the grid point. If the average was taken for less than 4 points, the wave height change was found to be too sensitive to the local bottom configuration. When the breaking wave condition was calculated, the local beach slope was defined as $(h'_j - h'_{j-10})/10 \Delta x$. This calculation predicted a reasonable breaking point. These procedures are believed to be reasonable because a transforming wave should be affected by the average value of the water depth in the vicinity of a given location.

3. COMPARISON WITH LABORATORY DATA

Three sets of laboratory experiments were performed to obtain data for comparison with the simulation model. The experimental conditions are shown in Table 2. During the experiments, the bottom profile, near bottom velocity and surface profile were measured. In order to measure the near bottom velocity, polystyrene particles were injected and a 16 mm camera was used to record their movement.

Figures 8(a) to (c) show the experimental results for the beach profile change and the corresponding results of the simulation. The model did not reach an equilibrium profile. The definition of equilibrium profile here is that there are no net sediment transport over the whole beach section. Even in laboratory

experiments in a wave flume, however, one cannot obtain an equilibrium profile for an erosional type beach ; the beach continues to erode, but at a slower rate.

The three simulation results exhibit the same tendencies as the corresponding laboratory re-

Table 2 Experimental condition for beach profile change.

Case	Wave Period (s)	Deep Water Wave Height (cm)	Deep Water Wave Steepness	Sediment Diameter (mm)	Initial Slope
1	1.5	10.6	0.036	0.2	0.1
2	1.2	6.2	0.028	0.2	0.05
3	1.5	9.3	0.027	0.7	0.1

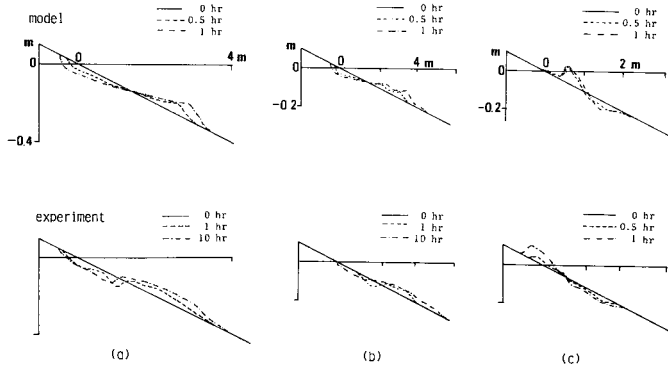


Fig. 8 Comparison of model and measured beach profile, (a) Case 1, (b) Case 2, (c) Case 3.

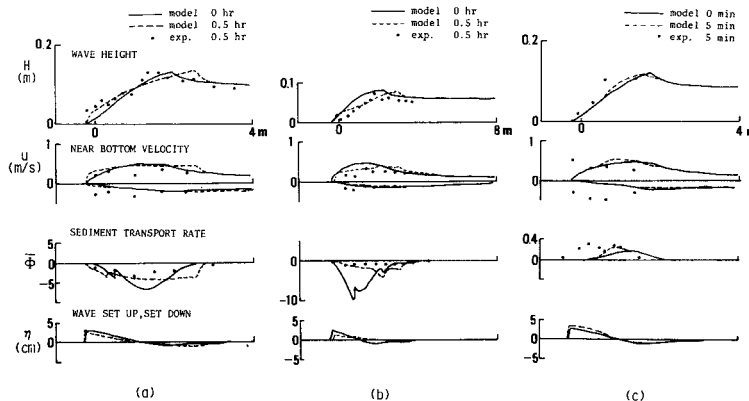


Fig. 9 Comparison between model and measured values, (a) Case 1, (b) Case 2, (c) Case 3.

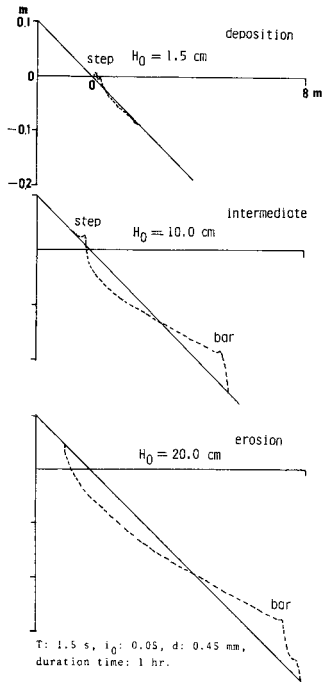


Fig. 10 Beach profile calculation for different wave height.

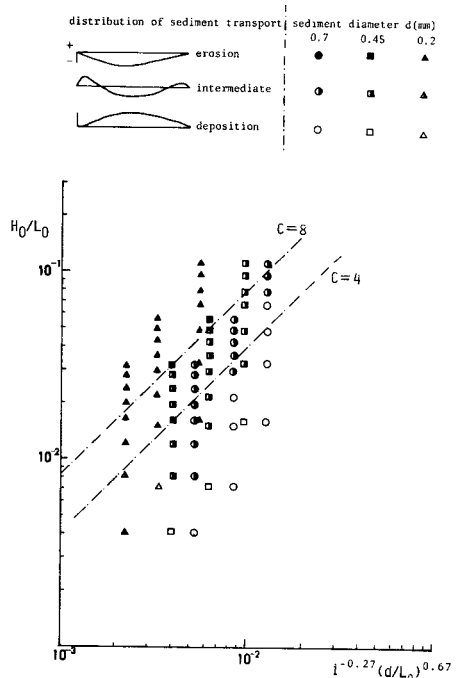


Fig. 11 Simulation results of beach pattern.

sults, i. e., an erosional beach or a depositional beach, but the small scale structures such as locations and heights of steps, troughs or bars are different. In order to find the reason for this discrepancy, Figs. 9(a) to (c) are given for the purpose of detailed comparisons between the calculated and measured wave heights, near bottom velocities, and transport rates.

It can be observed that the near bottom velocity field in the model does not always agree with the measured one, giving overestimated values for onshore and underestimated value for offshore in the surf zone. As a result, the model gives larger values for the transport rate as compared to the measurements in the surf zone. This is attributed to an overestimate in the wave height in the surf zone and to the velocity formulas, Eqs. (6) and (7). Moreover, the return flow is not included in the model, which may also lead to unrealistic results.

Figure 10 shows the change of resultant beach profile according to the wave height change for a fixed bed material (the diameter of which is 0.45 mm), bottom slope(0.05) and wave period(1.5 s). It can be observed that as the wave height increases, the resultant beach profile changes from depositional to intermediate and from intermediate to erosional.

Figure 11 shows the estimate of global patterns of beach profile, i. e., erosional, depositional and their intermediate types. The present model was applied for the combinations of three sand diameters (0.2 mm, 0.45 mm, 0.7 mm), three wave periods (1 s, 1.5 s, 2 s), eight deep water wave heights (2.5 cm, 5 cm, 7.5 cm, 10 cm, 12.5 cm, 15 cm, 17.5 cm, 20 cm) and one beach slope (0.05). In total 72 cases were calculated. In three cases of which wave period was 1 s and the deep water wave height was 20 cm, the wave steepness was so high that no wave existed for such conditions. Therefore 69 results for the distributions of sediment transport rate at the initial stage were obtained. The beach type was classified into three according to the distribution pattern as shown in the figure.

Sunamura and Horikawa⁽⁸⁾ have proposed a nondimensional parameter C^* which classifies the limiting boundaries for these types. The definition of C^* is

$$C^* = \frac{H_0}{L_0} i^{0.27} \left(\frac{L_0}{d} \right)^{0.67} \dots\dots\dots (17)$$

Their boundaries $C^*=4$ (deposition to intermediate), $C^*=8$ (intermediate to erosion) are also drawn in the figure. It seems that the intermediate type exists at the lower values of C^* than their boundary. However the present result seems reasonable since even in the original paper of Sunamura and Horikawa¹⁸⁾, the data scattering was not small.

The results of the model are encouraging for predicting the general tendency of the beach transformation, except for the surf zone. In the surf zone, the action of wave breaking is very strong and the wave motion becomes highly turbulent. The agitation due to breaking waves suspends the bed material, and the concentration of the suspended sediment in the vicinity of breaking point is high. The detailed discussions on this problem was presented by Shibayama and Horikawa¹⁹⁾.

4. CONCLUSIONS

The simplified calculation procedure to simulate two-dimensional beach transformation was proposed based on the recent results on wave transformation, near bottom velocity field and sediment transport. The agreement with the laboratory results was reasonably good to estimate global patterns. The reasons for the disagreement of small scale structures were also considered. The following two effects are considered to be most important and should be included in the next step.

- (1) the effect of large scale vortex created by wave breaking and
- (2) the complex nature of velocity field in the surf zone such as the return flow, wave reflection and small scale vortex.

REFERENCES

- 1) Mizuguchi, M. : An Heuristic Model of Wave Height Distribution in Surf Zone, Proc. 17th Coastal Eng. Conf., Vol. 1, pp. 278~289, 1980.
- 2) Koyama, Y. and Iwata, K. : A Method to Calculate Water Velocity in Shallow Water Region, Proc. 38th Annual Conf. of JSCE, Vol. II, pp. 303~304, 1983 (in Japanese).
- 3) Shibayama, T. and Horikawa, K. : Sediment Transport and Beach Transformation due to Waves, Proc. 18th Coastal Eng. Conf., pp. 1439~1458, 1982.
- 4) Shibayama, T. and Horikawa, K. : Bed Load Measurement and Prediction of Two-Dimensional Beach Transformation, Coastal Eng. in Japan Vol. 23, pp. 179~190, 1980.
- 5) Sunamura, T. : A Laboratory Study of Offshore Transport of Sediment and A Model for Eroding Beaches, Proc. 17th Coastal Eng. Conf., pp. 1051~1070, 1980.
- 6) Mizuguchi, M. and Mori, M. : Modeling of Two-Dimensional Beach Transformation due to Waves, Coastal Eng. in Japan, Vol. 24, pp. 155~170, 1981.
- 7) Isobe, M. and Horikawa, K. : On the Shallow Water Deformation of Velocity Field in the Surf-Zone, Proc. 28th Japanese Conf. on Coastal Eng., pp. 5~9, 1981 (in Japanese).
- 8) Goda, Y. : Deformation of Irregular Waves due to Depth-Controlled Wave Breaking, Report of the Port and Harbour Research Institute, Vol. 14, No. 3, 1975.
- 9) Watanabe, A., Isobe, M., Nozawa, K. and Horikawa, K. : Experimental Study on Bottom Velocity in the Nearshore Zone, Proc. 27th Japanese Conf. Coastal Eng., pp. 40~44, 1980 (in Japanese).
- 10) Horikawa, K., Watanabe, A. and Katori, S. : Sediment Transport under Sheet Flow Condition, Proc. 18th Coastal Eng. Conf., pp. 1335~1352, 1982.
- 11) Carstens, M. R., Neilson, F. M. and Altinbilek, H. D. : Bed Forms Generated in the Laboratory under an Oscillatory Flow, CERC. Tech. Memo., No. 28, 1969.
- 12) Shibayama, T. and Horikawa, K. : Laboratory Study on Sediment Transport Mechanism due to Wave Action, Proc. JSCE, No. 296, pp. 131~142, 1980.
- 13) Sawamoto, M., Yamashita, T. and Kitamura, T. : Distribution of Turbulence Intensity and Suspended Sediment Concentration over Rippled Bed, Proc. 28th Japanese Conf. on Coastal Eng., pp. 232~236, 1981 (in Japanese).
- 14) Kennedy, J. F. and Falcon, N. N., : Wave-Generated Sediment Ripples, MIT, Hydrodynamic Lab., Report No. 86, 55 p, 1965.
- 15) Allen, J. : Scale Models in Hydraulic Engineering, Longmans, Green and Co., p. 212, 1947.

- 16) Terzaghi, K. and Peck, R. : Soil Mechanics in Engineering Practice, John Wiley, p.185, 1973.
- 17) Shibayama, T. : Sediment Transport Mechanism and Two-Dimensional Beach Transformation due to Waves, Doctoral Dissertation Submitted to the Univ. of Tokyo, 159 p, 1984.
- 18) Sunamura, T. and Horikawa, K. : Two-dimentional Beach Transformation due to Waves, Proc. 14th Coastal Eng. Conf., pp.920~938, 1974.
- 19) Shibayama, T. and Horikawa, K. : Sediment Suspension due to Breaking Waves, Coastal Eng. in Japan, Vol.25, pp.163~176, 1982.

(Received June 6 1984)
